

AD-A036 124

ARMY ELECTRONICS COMMAND FORT MONMOUTH N J
APPLICATION OF BETHE'S THEORY ON ELECTRON SCATTERING TO E-BEAM --ETC(U)
FEB 77 6 J IAFRATE, J N HELBERT, A D BALLATO

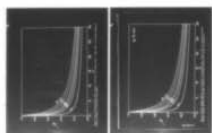
F/G 20/7

UNCLASSIFIED

ECOM-4466

NL

1 OF 1
AD
A036124



END

DATE
FILMED
3-77



ADA 036124



✓

12
B.S.

Research and Development Technical Report
ECOM - 4466

**APPLICATION OF BETHE'S THEORY ON ELECTRON
SCATTERING TO E-BEAM LITHOGRAPHY**

**Gerald J. Iafrate
John N. Helbert
Arthur D. Ballato
Electronics Technology & Devices Laboratory
and**

**Walter S. McAfee
Research, Development & Engineering Directorate**

February 1977

**DISTRIBUTION STATEMENT
Approved for public release;
distribution unlimited.**

**D D C
RECEIVED
MAR 1 1977
RECEIVED**

[Handwritten signature] A

ECOM

US ARMY ELECTRONICS COMMAND FORT MONMOUTH, NEW JERSEY 07703

NOTICES

Disclaimers

The findings in this report are not to be construed as an official Department of the Army position, unless so designated by other authorized documents.

The citation of trade names and names of manufacturers in this report is not to be construed as official Government indorsement or approval of commercial products or services referenced herein.

Disposition

Destroy this report when it is no longer needed. Do not return it to the originator.

UNCLASSIFIED

SECURITY CLASSIFICATION OF THIS PAGE (When Data Entered)

REPORT DOCUMENTATION PAGE		READ INSTRUCTIONS BEFORE COMPLETING FORM
1. REPORT NUMBER ECON-4466 ✓	2. GOVT ACCESSION NO.	3. RECIPIENT'S CATALOG NUMBER
4. TITLE (and Subtitle) APPLICATION OF BETHE'S THEORY ON ELECTRON SCATTERING TO E-BEAM LITHOGRAPHY		5. TYPE OF REPORT & PERIOD COVERED
6. AUTHOR(s) Gerald J. Iafrate, Walter S. McAfee John N. Helbert, ETDL RD/E Dir Arthur D. Ballato		6. PERFORMING ORG. REPORT NUMBER
7. PERFORMING ORGANIZATION NAME AND ADDRESS Electronic Materials Research Technical Area US Army Electronics Technology & Devices Lab (ECON) Fort Monmouth, NJ 07703 DRSEL-TL-ESH		8. CONTRACT OR GRANT NUMBER(s)
11. CONTROLLING OFFICE NAME AND ADDRESS US Army Electronics Command Fort Monmouth, NJ 07703 DRSEL-TL-ESH		10. PROGRAM ELEMENT, PROJECT, TASK AREA & WORK UNIT NUMBERS 61102A ILI61192AH47 S7/041
12. MONITORING AGENCY NAME & ADDRESS (if different from Controlling Office) Research and development technical rept.		12. REPORT DATE February 1977
16. DISTRIBUTION STATEMENT (of this Report) Approved for public release; distribution unlimited.		13. NUMBER OF PAGES 5
17. DISTRIBUTION STATEMENT (of the abstract entered in Block 20, if different from Report)		14. SECURITY CLASS. (of this report) Unclassified
18. SUPPLEMENTARY NOTES		15a. DECLASSIFICATION/DOWNGRADING SCHEDULE 12/22p.
19. KEY WORDS (Continue on reverse side if necessary and identify by block number) Electron Scattering E-Beam Lithography E-Beam Undercutting Polymers		
20. ABSTRACT (Continue on reverse side if necessary and identify by block number) In this report, attention is focused on the question of the spatial extent developed by an intermediate energy (5-20 keV) scattered electron beam in a lithographic e-beam resist material. Use is made of the multiple scattering theory of Bethe to calculate the average cosine between the actual direction of motion and the direction of the primary electron beam in terms of the average nuclear charge of the target and the depth of electron penetration into the target. Use is made of the average cosine calculation to establish an order-of-magnitude expression for the depth at which two electron-beam lines overlap to cause undercutting.		

REPORT DOCUMENTATION PAGE	
1. REPORT NUMBER	
2. AUTHOR	
3. TITLE	
4. NUMBER OF PAGES	
5. PRICE	
6. AUTHORING ORGANIZATION NAME(S)	
7. AUTHORING ORGANIZATION REPORT NUMBER	
8. PERFORMING ORGANIZATION NAME(S)	
9. PERFORMING ORGANIZATION REPORT NUMBER	
10. CONTRACT OR GRANT NUMBER(S)	
11. DISTRIBUTION STATEMENT (See Instructions for Authors)	
12. DISTRIBUTION STATEMENT (See Instructions for Authors)	
13. DISTRIBUTION STATEMENT (See Instructions for Authors)	
14. DISTRIBUTION STATEMENT (See Instructions for Authors)	
15. DISTRIBUTION STATEMENT (See Instructions for Authors)	
16. DISTRIBUTION STATEMENT (See Instructions for Authors)	
17. DISTRIBUTION STATEMENT (See Instructions for Authors)	
18. DISTRIBUTION STATEMENT (See Instructions for Authors)	
19. DISTRIBUTION STATEMENT (See Instructions for Authors)	
20. DISTRIBUTION STATEMENT (See Instructions for Authors)	
21. DISTRIBUTION STATEMENT (See Instructions for Authors)	
22. DISTRIBUTION STATEMENT (See Instructions for Authors)	
23. DISTRIBUTION STATEMENT (See Instructions for Authors)	
24. DISTRIBUTION STATEMENT (See Instructions for Authors)	
25. DISTRIBUTION STATEMENT (See Instructions for Authors)	
26. DISTRIBUTION STATEMENT (See Instructions for Authors)	
27. DISTRIBUTION STATEMENT (See Instructions for Authors)	
28. DISTRIBUTION STATEMENT (See Instructions for Authors)	
29. DISTRIBUTION STATEMENT (See Instructions for Authors)	
30. DISTRIBUTION STATEMENT (See Instructions for Authors)	
31. DISTRIBUTION STATEMENT (See Instructions for Authors)	
32. DISTRIBUTION STATEMENT (See Instructions for Authors)	
33. DISTRIBUTION STATEMENT (See Instructions for Authors)	
34. DISTRIBUTION STATEMENT (See Instructions for Authors)	
35. DISTRIBUTION STATEMENT (See Instructions for Authors)	
36. DISTRIBUTION STATEMENT (See Instructions for Authors)	
37. DISTRIBUTION STATEMENT (See Instructions for Authors)	
38. DISTRIBUTION STATEMENT (See Instructions for Authors)	
39. DISTRIBUTION STATEMENT (See Instructions for Authors)	
40. DISTRIBUTION STATEMENT (See Instructions for Authors)	
41. DISTRIBUTION STATEMENT (See Instructions for Authors)	
42. DISTRIBUTION STATEMENT (See Instructions for Authors)	
43. DISTRIBUTION STATEMENT (See Instructions for Authors)	
44. DISTRIBUTION STATEMENT (See Instructions for Authors)	
45. DISTRIBUTION STATEMENT (See Instructions for Authors)	
46. DISTRIBUTION STATEMENT (See Instructions for Authors)	
47. DISTRIBUTION STATEMENT (See Instructions for Authors)	
48. DISTRIBUTION STATEMENT (See Instructions for Authors)	
49. DISTRIBUTION STATEMENT (See Instructions for Authors)	
50. DISTRIBUTION STATEMENT (See Instructions for Authors)	

CONTENTS

	Page
INTRODUCTION	1
THEORY AND RESULTS	2
FIGURES	
1. Plot of $\langle \cos\theta \rangle$ [Eq. (7)] as a function of the average nuclear charge Z ; normalized depth, y_d , is treated as a parameter.	4
2. Plot of $\langle \cos\theta \rangle$ [Eq. (4) numerically integrated] as a function of the average nuclear charge Z ; incident electron accelerating voltage V_0 , and normalized depth, y_d , are treated as parameters.	5
3. Diagram depicts two e-beams, separated by a distance, D , striking the target; the geometrical angle, θ_g , and the undercutting length, L , are visually defined.	7
4. Plot of reduced depth, f [Eq. (8)], as a function of average nuclear charge Z ; D , the reduced separation between e-beams, is treated as a parameter.	8
5. Plot of reduced depth, f , as a function of average nuclear charge Z ; D , the reduced separation between e-beams, and V_0 , the incident electron accelerating voltage, are treated as parameters.	9

ACCESSION FOR	
918	Write Section <input checked="" type="checkbox"/>
722	Draft Section <input type="checkbox"/>
UNANNOUNCED JUSTIFICATION <input type="checkbox"/>	
BY	
DISTRIBUTION/AVAILABILITY CODE	
DATE	INITIALS

APPLICATION OF BETHE'S THEORY ON ELECTRON SCATTERING TO E-BEAM LITHOGRAPHY

INTRODUCTION

Electron-beam lithography (EBL) is a technique which makes possible the fabrication of integrated circuits with faster operating times, higher production reliability, lower cost per electric function, and greater packing densities.¹ EBL relies heavily upon polymer resists for pattern delineation as does the more conventional photolithography technique. Many papers have been written concerning e-beam resist sensitivities,² but little attention has been given to scattering phenomena in the polymer resist layer and the effect of this scattering on line undercutting or resolution. Several papers have appeared which treat electron backscattering from underlying substrates,³ but electron scattering in the upper layer resist as a possible phenomenon governing integrated circuit (IC) feature oversizing has been overlooked. This topic assumes greater importance in the light of recent work on high atomic-numbered (Z) acrylic polymer resist compositions by workers at IBM.⁴ These workers studied thallium (Tl) and cesium (Cs) substituted methacrylic acid copolymers which have average atomic numbers (Z) higher than the Z-values of well-known resist polymers. Typical Z values for well-known resist polymers are 2.6 for poly(isobutylene), 3.6 for poly(methyl methacrylate) (PMMA), 4.1 for poly(butene-1-sulfone), while the value for 100% Cs-substituted homopolymer $\left[\text{CH}_2 - \underset{\text{COOCs}}{\text{C}}(\text{CH}_3) \right]_n$ is 11. Since electron scattering phenomena are Z-dependent,

electron scattering in higher-Z polymer resists is an important topic. Assuming lack of limited freedom in the selection of the substrate and a fixed degree of substrate backscattering, electron scattering in the resist becomes a factor governing pattern resolution.

In EBL, an intermediate energy (5-20 keV) electron beam exposes a radiation sensitive target (such as the polymer PMMA) overlaid on an IC substrate; a subsequent chemical development treatment removes the exposed region leaving an outline of pattern sketched by the electron beam when employing a positive-acting resist. The electron-beam technique is attractive because it leads to the production of micron to submicron resolved channels and also lends itself to computer-controlled production line automation. However, the use of an electron beam does introduce certain difficulties in that electrons penetrating the target scatter away from the incident electron beam and cause intended exposure to other regions of the target. This scattering leads to a widening and distortion of the exposed region and results in a degradation of the resolution of two parallel electron-beam lines. Therefore, an appreciation for the spatial extent of penetrating electrons scattered from an incident electron beam is central to the implementation of electron-beam lithography.

-
1. A.L. Robinson, *Science*, 189, 540 (1975).
 2. L.F. Thompson, *Solid State Technology*, Part 1, 27, July (1974).
 3. R.J. Hawryluk, Tech. Report 511, Lincoln Laboratory, MIT (1974).
 4. R. Feder, T. Haller, M. Hatzakis, L.T. Romankiw, and E. Spiller, *IBM Technical Disclosure Bulletin*, 18, 2346 (1975).

In this report, we address, qualitatively, the question of the spatial extent of scattered electrons. We do this by making use of the multiple scattering theory of Bethe et al.^{5,6} to calculate the average cosine between the actual direction of motion and the direction of the primary electron beam in terms of the average nuclear charge of the target and the depth of electron penetration into the target. Moreover, we make use of the average-cosine calculation to establish an order-of-magnitude expression for the depth L at which two electron-beam lines overlap in terms of the average nuclear charge of the target.

THEORY AND RESULTS

Bethe et al. (see footnotes 5 and 6, page 2) established the average cosine between the actual direction of motion and the direction of the primary beam for fast electrons to be

$$\langle \cos\theta \rangle = \exp \left[(-2) \int_{E_d}^{E_0} \frac{dE}{\lambda \left| \frac{dE}{dx} \right|} \right] \quad (1)$$

where λ is the "transport mean free path," $\left| \frac{dE}{dx} \right|$ is the energy loss law for primary electrons moving through the target, E_0 is the incident electron energy, and E_d is the energy of electrons at depth d . Both λ and $\left| \frac{dE}{dx} \right|$ are given by

$$\frac{1}{\lambda} = \frac{\pi N e^4 Z^2}{2E^2} \ln \left[\frac{2a_H m (2E/m)^{1/2}}{N Z^{1/3}} \right] \quad (2)$$

and

$$\left| \frac{dE}{dx} \right| = 2\pi N e^4 Z \frac{\ln(2E/J)}{E} \quad (3)$$

where N is the number of target atoms per cc, Z is the average nuclear charge of the target, and a_H is the radius of the first Bohr orbit (e and m are, of course, the charge and rest mass of the electron). J , generally referred to as the mean excitation energy of the solid, is given as $J=11.5 Z$ eV in this calculation although it is assumed to have a different value in polymer targets (see footnote 3, page 1). In substituting Eqs. (2,3) into Eq. (1) and letting $E=eV$, we obtain the expression for $\langle \cos\theta \rangle$ as

$$\langle \cos\theta \rangle = \exp \left[\left(-\frac{1}{2}Z\right) \int_{V_d}^{V_0} \left[I(V,Z)/V \right] dV \right] \quad (4a)$$

5. H. Bethe, Rose, and Smith, Proc. American Philosophical Society, 78, p. 573 (1938).

6. H. Bethe, Ann. Physik, 5, p. 325 (1930).

where

$$I(V,Z) = \frac{\ln(0.54 V^{1/2}/Z^{1/3})}{\ln(0.174 V/Z)} \quad (4b)$$

We note that, I , the ratio of the logarithms in the integrand of Eq. (4), is a slowly varying function of Z and V for $Z \gtrsim 1$ and $V \gtrsim 5$ kV. G. Archard,⁷ in obtaining his electron backscattering coefficient for the situation that Bethe (see footnote 5, page 2) termed "complete diffusion," used the approximation that $I \simeq 0.7$ which is quite accurate for $10 \lesssim Z \lesssim 80$ and for $5 \text{ kV} \lesssim V_0$, $V_d \lesssim 50$ kV and is even fairly accurate for $1 \lesssim Z \lesssim 80$. Using Archard's approximation in the expression for the $\langle \cos\theta \rangle$ of Eq. (4) results in

$$\langle \cos\theta \rangle = (V_d/V_0)^{7Z/20} \quad (5)$$

The energy, eV_d , can be obtained in terms of the depth of penetration, d , and the incident electron energy, eV_0 , by integrating Eq. (3) over the appropriate limits. Following G. Archard (see footnote 7, page 3), we find, to a reasonable approximation, that

$$(V_d/V_0) = (1 - d/R)^{1/2} \quad (6)$$

where R is the range of the electrons and is dependent upon the target material parameters and the incident electron energy. It then follows from Eqs. (5,6) that the $\langle \cos\theta \rangle$ can be approximated by

$$\langle \cos\theta \rangle = (1 - y_d)^{7Z/40} \quad (7a)$$

$$y_d = d/R. \quad (7b)$$

In Figure 1, we plot the $\langle \cos\theta \rangle$ of Eq. (7a) as a function of the average nuclear charge Z while treating the normalized depth, y_d , as a parameter. We note that the $\langle \cos\theta \rangle$ as given by Eq. (7) is independent of incident electron energy.* Indeed, upon performing the integration of Eq. (4) while using V_d in Eq. (6) for a lower limit, we obtain the numerical result for $\langle \cos\theta \rangle$ as displayed in Figure 2. We note that there is a slight incident energy dependence as well as a slight shift to higher values for the numerically integrated $\langle \cos\theta \rangle$ plotted in Figure 2. Nonetheless, a comparison of the results in Figures 1 and 2 shows similar qualitative behavior for the $\langle \cos\theta \rangle$.

One can make use of the $\langle \cos\theta \rangle$ calculation to establish the dependence of the undercutting on target nuclear charge of two equally exposed parallel electron-beam lines. We define, somewhat arbitrarily, L , as the depth at which electrons scattered from each beam mutually expose the region of the target midway between the two electron-beam lines. The depth L is then determined by setting the $\langle \cos\theta \rangle$ equal to the geometrical cosine;

7. G. Archard, J. Appl. Phys., 32, p. 1505 (1961).

* The incident electron energy appears in the expression for the electron range, R , which is model-dependent; this model dependence arises from the fact that Eq. (6) can be derived, not only as an approximation to Bethe's energy loss law, but also from the Thomson-Widdington energy loss law.

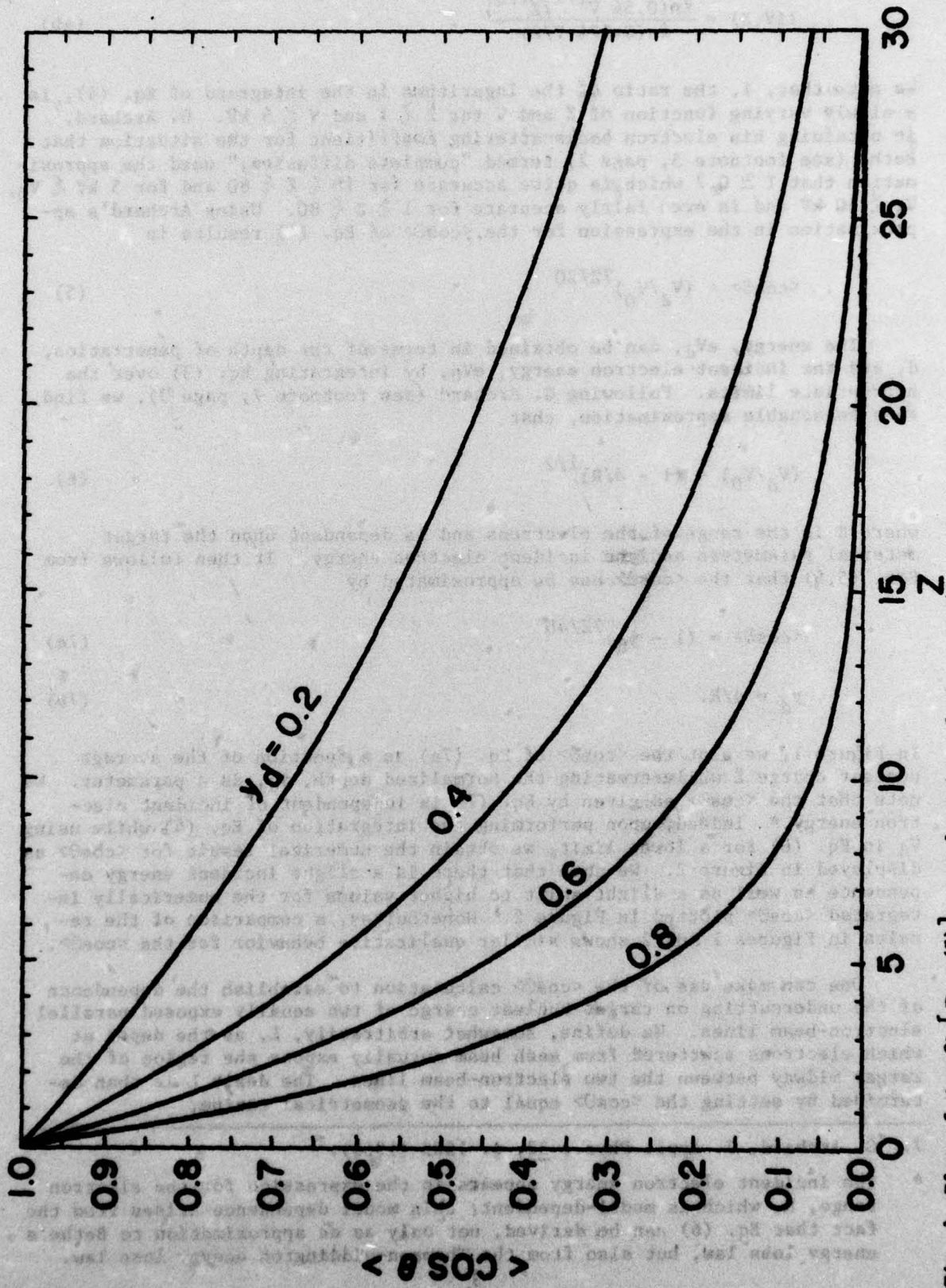


Fig. 1. Plot of $\langle \cos\theta \rangle$ [Eq. (7)] as a function of the average nuclear charge Z ; normalized depth, y_d , is treated as a parameter.

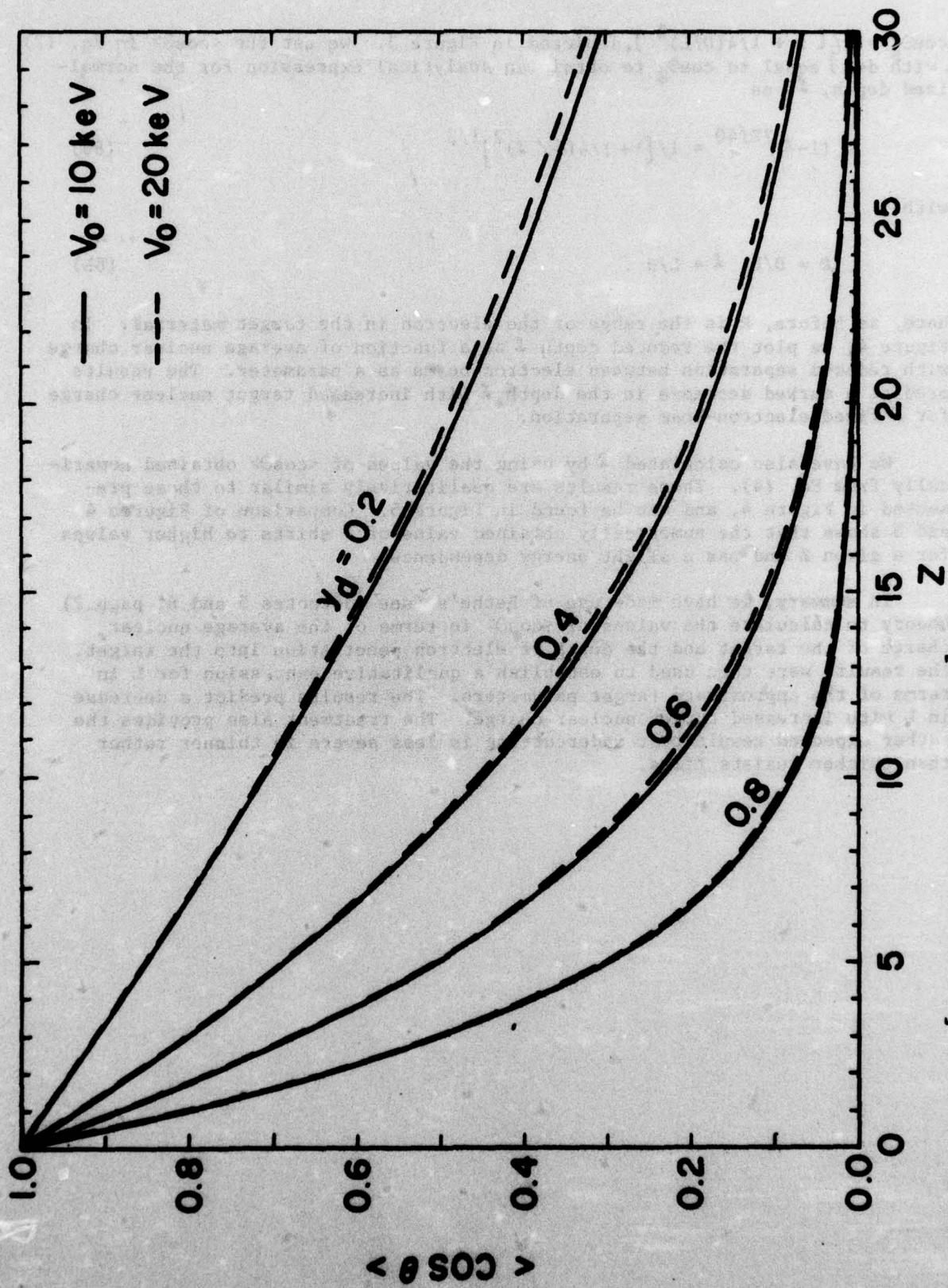


Fig. 2. Plot of $\langle \cos \theta \rangle$ [Eq. (4) numerically integrated] as a function of the average nuclear charge Z ; incident electron accelerating voltage, V_0 , and normalized depth, y_d , are treated as parameters.

$\cos\theta_g = 1/[1 + 1/4(D/L)^2]$, depicted in Figure 3. We set the $\langle\cos\theta\rangle$ in Eq. (7) [with $d=L$] equal to $\cos\theta_g$ to obtain an analytical expression for the normalized depth, f , as

$$(1-f)^{7Z/40} = 1/[1 + 1/4(D/L)^2]^{1/2} \quad (8a)$$

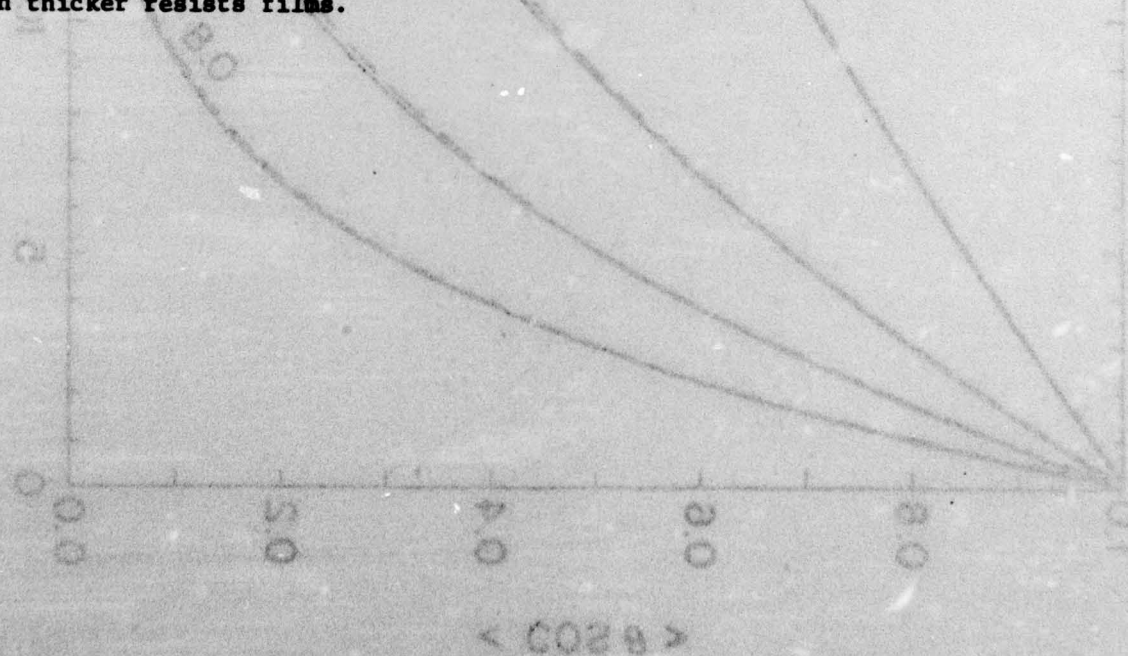
with

$$D = D/R, \quad f = L/R. \quad (8b)$$

Here, as before, R is the range of the electron in the target material. In Figure 4, we plot the reduced depth f as a function of average nuclear charge with reduced separation between electron beams as a parameter. The results predict a marked decrease in the depth f with increased target nuclear charge for a fixed electron-beam separation.

We have also calculated f by using the values of $\langle\cos\theta\rangle$ obtained numerically from Eq. (4). These results are qualitatively similar to those presented in Figure 4, and can be found in Figure 5. Comparison of Figures 4 and 5 shows that the numerically obtained value of f shifts to higher values for a given Z and has a slight energy dependence.

In summary, we have made use of Bethe's (see footnotes 5 and 6, page 2) theory to calculate the values of $\langle\cos\theta\rangle$ in terms of the average nuclear charge of the target and the depth of electron penetration into the target. The results were then used to establish a qualitative expression for L in terms of the approximate target parameters. The results predict a decrease in L with increased target nuclear charge. The treatment also provides the rather expected result that undercutting is less severe in thinner rather than thicker resists films.



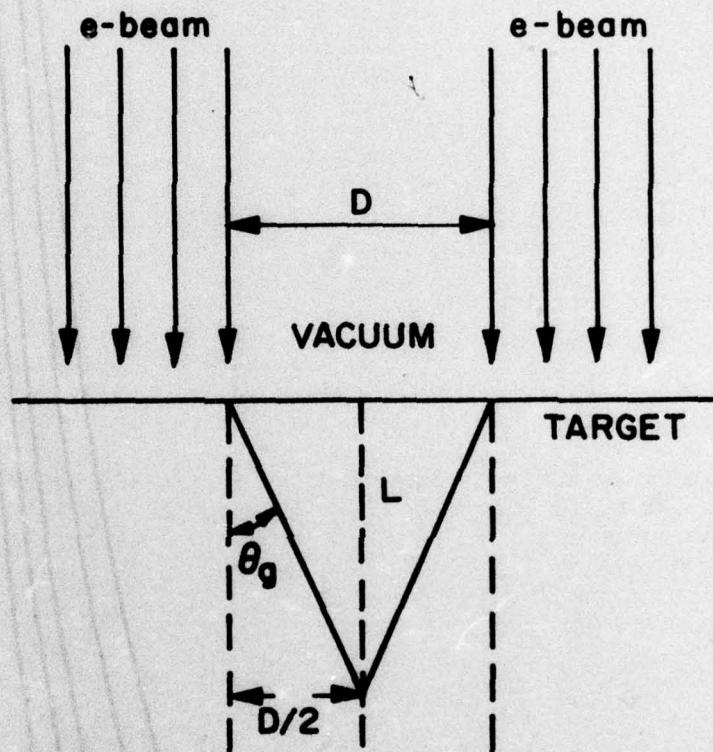


Fig. 3. Diagram depicts two e-beams, separated by a distance, D , striking the target; the geometrical angle, θ_g , and the undercutting length, L , are visually defined.

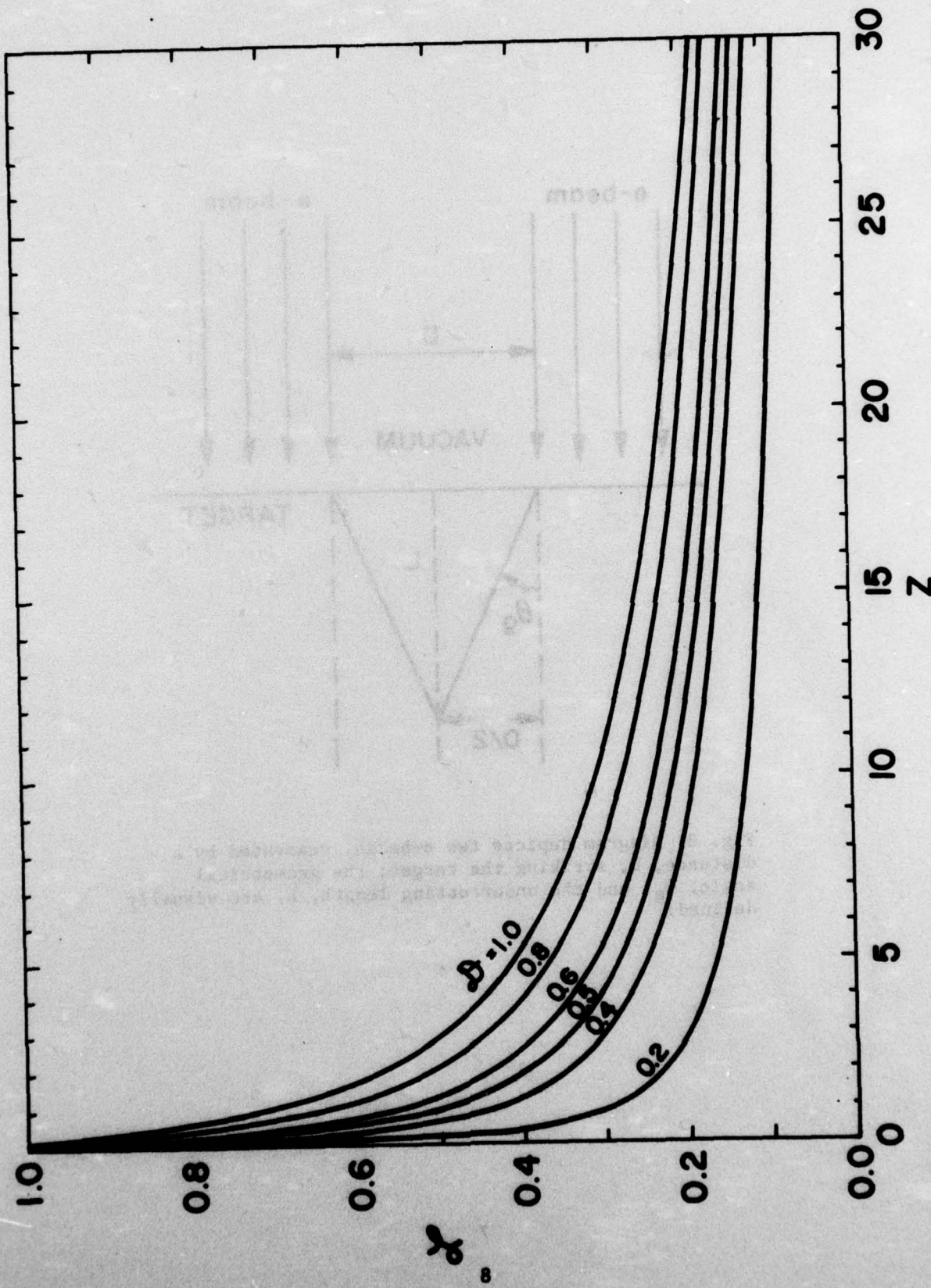


Fig. 4. Plot of reduced depth, z [Eq. (8)], as a function of average nuclear charge Z ; D , the reduced separation between e-beams, is treated as a parameter.

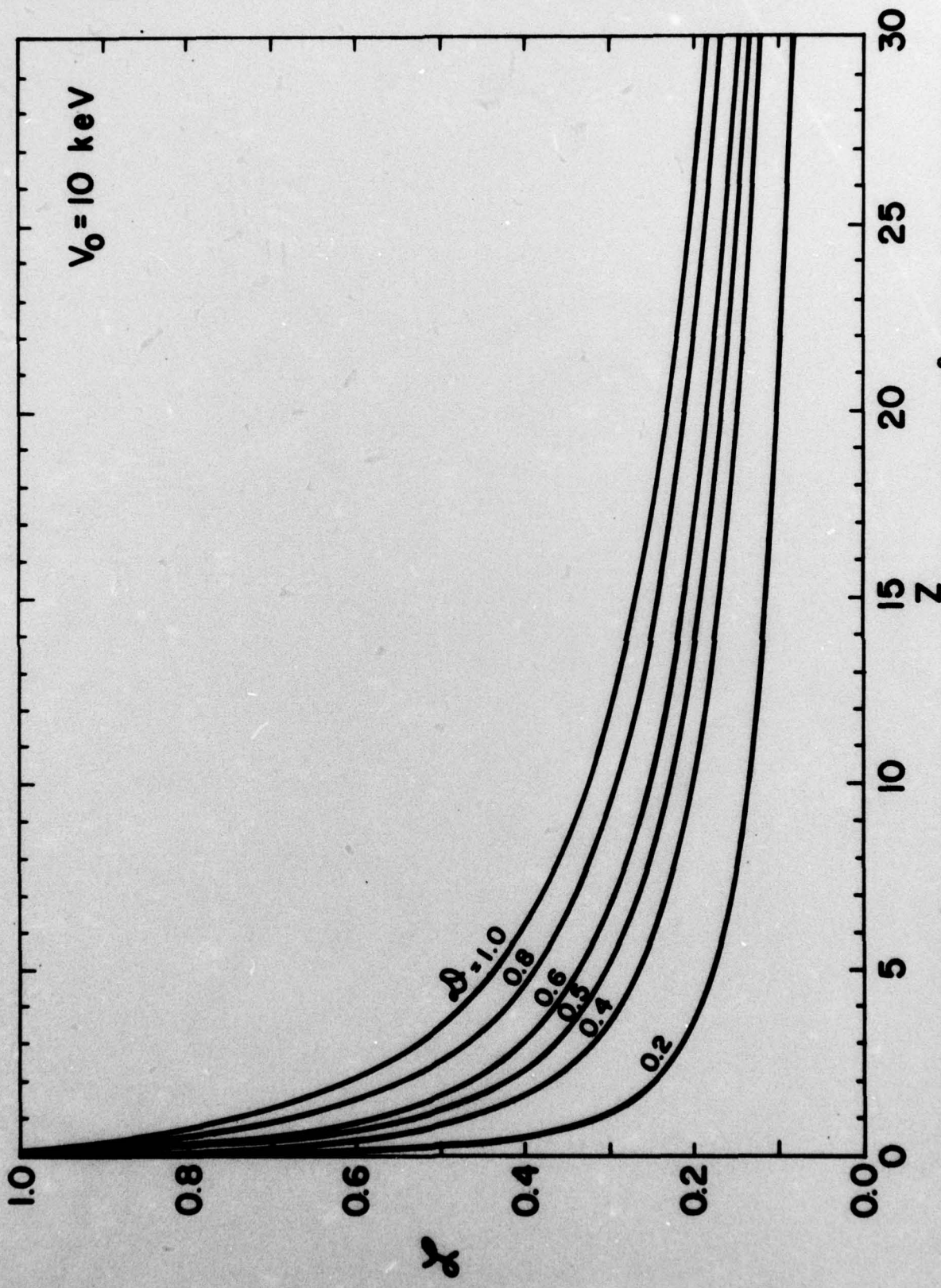


Fig. 5. Plot of reduced depth, \bar{z} , as a function of average nuclear charge Z ; \bar{D} , the reduced separation between e-beams, and V_0 , the incident electron accelerating voltage, are treated as parameters.